

Multiscale Detection of Curvilinear Structures in 2-D and 3-D Image Data

Th. M. Koller, G. Gerig, G. Székely, and D. Dettwiler

Communication Technology Laboratory, Image Science,
ETH-Zentrum, CH-8092 Zurich, Switzerland
e-mail: tkoller{gerig,szekely}@vision.ee.ethz.ch

Abstract

This paper presents a novel, parameter-free technique for the segmentation and local description of line structures on multiple scales, both in 2-D and 3-D. The algorithm is based on a nonlinear combination of linear filters and searches for elongated, symmetric line structures, while suppressing the response to edges. The filtering process creates one sharp maximum across the line-feature profile and across scale-space. The multiscale response reflects local contrast and is independent of the local width.

The filter is steerable in orientation and scale domain, leading to an efficient, parameter-free implementation. A local description is obtained that describes the contrast, the position of the center-line, the width, the polarity, and the orientation of the line.

Examples of images from different application domains demonstrate the generic nature of the line segmentation scheme. The 3-D filtering is applied to magnetic resonance volume data in order to segment cerebral blood vessels.

1 Introduction

The famous Greek mathematician and philosopher Euclid defined a line as “what has a length, but no width”. The quotation illustrates the most significant feature of a line: it is extended in one direction and its width is small: a *line* is a 1-dimensional manifold.

Early algorithms for the detection of such structures tried to find roads in aerial imagery with nonlinear small pixel operators [4, 13] by looking at sequences of pixels which were brighter or darker than the background. Haralick [7] proposed to fit the pixel intensities in local neighborhoods by a continuous parametric surface and to evaluate its derivatives. These methods, however, did not sufficiently take into account that line structures can be represented at different scales. A river on a local map will be a wide band, but on a large scale map it might be a thin line.

Canny [1, 2] proposed an ‘optimal’ ridge detector and introduced scale as an essential parameter, but he could not solve the problem of integrating the filter responses from different scales.

The simultaneous detection of edges and lines was approached by proposing energy filters [11, 12]. Discrimination between the two types of features can be done by calculating the phase information, but this is much more sensitive to noise than the filter itself. Multiscale properties of quadratic edge detectors were studied by Kube et al. [9, 10].

Another class of papers studied the properties of multiscale ridges [6], generating watersheds on multiple scales followed by ridge detection in the $n + 1$ dimensional space. Structures were sought by multidimensional differentiation in scale space.

Subirana et al. [14] proposed an interesting concept for multiscale ridge analysis. They achieved scale integration of 1-D ridge segmentation by looking at the minimum of two shifted filter responses. They applied the 1-D filter on 2-D images, but did not develop 2-D directional filters on multiple scales.

This paper proposes a new technique for the segmentation of lines at multiple scales. The basic idea comes close to the approach of Subirana et al., but is extended to 2-D and 3-D and aims at multiscale structure detection. The nonlinear combination of filters allows a true integration of scales as a projection, avoiding complex heuristic search strategies. It further suppresses filter response to single discontinuities completely and thus focuses on curvilinear features. The new line filtering scheme achieves more than only a characterization of line centers; it also extracts local shape attributes.

2 Multiscale line detection in 1-D

A simple line model

The goal of the filtering process is to detect curvilinear structures of arbitrary shape and not to attempt to distinguish between different *line-like* profiles, such as bars, roofs and smooth ridges. Additionally, the filtering should derive the width and height of the detected structures.

In the following discussion of the new line-filtering technique we use the bar-profile and will show later that the method works for other profiles as well. The bar-profile for a line centered at $x = 0$ with height 1

and width w can be expressed using the step-edge function $\Theta(x)$.

$$\text{Bar}(x) = \Theta(x + \frac{w}{2}) - \Theta(x - \frac{w}{2}), \quad \Theta(x) = \begin{cases} 1, & x > 0 \\ 0, & \text{else} \end{cases}$$

We first discuss linear filtering and derive an appropriate scaling to perform scale integration. Based on these results we can then develop the nonlinear segmentation scheme.

Scale integration with linear filtering

Canny [1] proposed to take the second derivative of the Gaussian function

$$\text{FLine}(x) = -c_\sigma G_\sigma''(x) = -c_\sigma \left(\frac{x^2}{\sigma^4} - \frac{1}{\sigma^2} \right) e^{-\frac{x^2}{2\sigma^2}}$$

as a filter and locate lines at points where the convolution of the function with the line profile has a maximum. $G_\sigma(x)$ denotes the unscaled Gaussian function $G_\sigma(x) = e^{-\frac{x^2}{2\sigma^2}}$, $G'_\sigma(x)$ and $G''_\sigma(x)$ its first and second derivatives in x , and c_σ a normalization function depending on σ . The convolution with a bar of width w gives the sum of two edge responses

$$\mathcal{R}\text{Line}_\sigma(x) = c_\sigma \left(G'_\sigma(x + \frac{w}{2}) - G'_\sigma(x - \frac{w}{2}) \right).$$

The condition that the response $\mathcal{R}\text{Line}$ has a maximum at $x = 0$, the center of the line, is $\sigma \geq \frac{\sqrt{3}}{6}w$.

Only an appropriate normalization allows a calculation of the height and width of the line from its filter response. With a polynomial $c_\sigma = a \cdot \sigma^n$ as the normalization function, the response at $x = 0$ is maximal if σ satisfies $\sigma = \pm \frac{w}{2\sqrt{2-n}}$. A solution exists only if $n < 2$. We substitute the optimal σ back into f to get

$$f(\sigma_{\text{opt}}) = aw^{n-1} \frac{1}{(2\sqrt{2-n})^{n-2}} e^{\frac{2-n}{2}}$$

as the response at $x = 0$ for the optimal σ_{opt} . This expression is independent of w if and only if $n = 1$. Setting $a = \frac{2}{\sqrt{e}}$ finally gives a value of h to a bar of height h .

This linear filter also gives a response to step-edges. The response is proportional to G'_σ , and has extrema at $\pm\sigma$, where the value is half the height of the step edge. Further, a line profile generates two side lobes of opposite sign to its main response near positions $-\frac{w}{2} + \sigma$ and $\frac{w}{2} - \sigma$. These multiple responses to lines and the sensitivity to step-edges does impede the application of a simple scale integration scheme, a problem that occurs for *every linear filter*.

Nonlinear multiscale line filtering

Although the linear filtering discussed above is not suitable for multiscale line detection, we can derive a new scheme from it. Since the second derivative of a

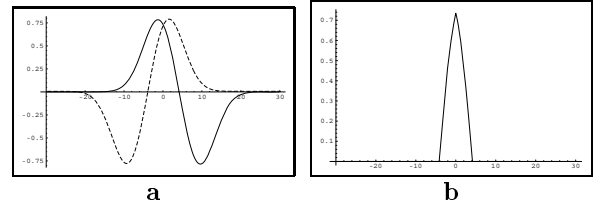


Figure 1: The responses of the left and right edge detectors \mathcal{R}_l and \mathcal{R}_r to a bar of width 10 (a). The nonlinear combination $\mathcal{R}_s(x)$ of the responses gives a sharp peak at the center of the bar (b).

function can be rewritten as a discrete derivative of the first derivative, the filter becomes

$$\text{FLine}(x) = -a\sigma \frac{G'_\sigma(x+h) - G'_\sigma(x-h)}{2h} + O(h^2)$$

with $h = \sigma = \frac{w}{2}$

$$\text{FLine}(x) \approx \frac{a}{2} \left(-G'_\sigma(x + \frac{w}{2}) + G'_\sigma(x - \frac{w}{2}) \right).$$

The first derivative of the Gaussian $G'_\sigma(x)$ is a well known edge detector [2]. The edge detectors $E_l = -G'_\sigma(x + \frac{w}{2})$ and $E_r = G'_\sigma(x - \frac{w}{2})$ detect the left and right edge of the bar profile at location $x = \mp \frac{w}{2}$ and place the output with a maxima at $x = 0$. After scaling and summing the outputs we get the response $\text{FLine} = \frac{a}{2}(E_l + E_r)$. Since $\frac{a}{2}$ is only a proportionality constant it will be omitted in the ensuing discussion.

To overcome the multiple line response and the sensitivity to edges, the convolution responses of the two shifted edge filters must be combined in a *nonlinear* way. The function $F(\mathcal{R}_l, \mathcal{R}_r)$ that calculates the final response must be large, if both \mathcal{R}_l and \mathcal{R}_r are large and zero if either \mathcal{R}_l or \mathcal{R}_r is zero. We choose the minimum operation $F(\mathcal{R}_l, \mathcal{R}_r) = \min(\mathcal{R}_l, \mathcal{R}_r)$. Another possible choice would be the geometrical mean $F(\mathcal{R}_l, \mathcal{R}_r) = \sqrt{\mathcal{R}_l \cdot \mathcal{R}_r}$.

Here, we come close to Subirana and Sung [14], who developed a “ridge detection scheme” based on a nonlinear combination of two shifted filters. However, they designed two asymmetric filters in order to handle regions with narrow adjacent regions.

The detectors E_l and E_r will also detect the opposite edges of a bar, but with inverse sign. Therefore we combine only the positive parts of \mathcal{R}_l and \mathcal{R}_r for the detection of positive bars. Introducing the function $\text{Pos}(x) = x \cdot \Theta(x)$, ($= x, x > 0$) and the shift s as a separate parameter we can write the result of the line filter at location x for a profile $f(x)$ as

$$\begin{aligned} \mathcal{R}_s(x) &= \min(\text{Pos}((E_l \otimes f)(x)), \text{Pos}((E_r \otimes f)(x))) \\ E_l(x) &= -G'_\sigma(x + s) \quad \text{and} \quad E_r(x) = G'_\sigma(x - s). \end{aligned}$$

The σ in this equation affects only the SNR of the

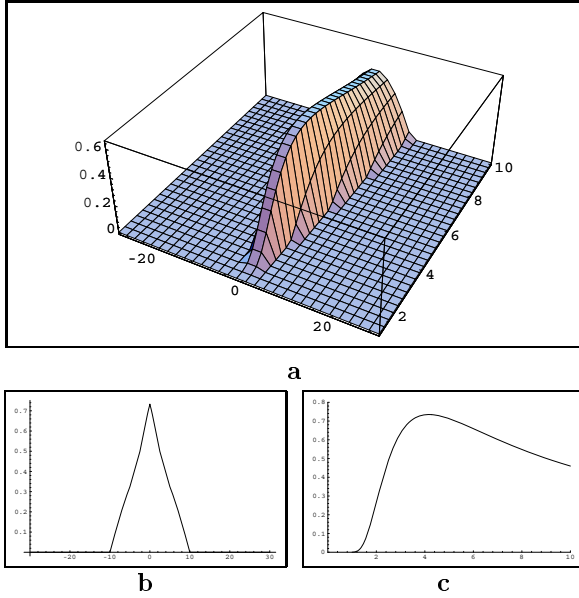


Figure 2: Scale space response of the nonlinear filtering to a bar of width 10 (a). The scale increases from front to back. Plots (b) and (c) show the maximum projection of the scale axis and the response at the center of the bar as a function of scale.

edge detectors E_l and E_r , whereas the shift s depends on the width w of the line. Consequently we want to choose σ as large as possible, but not larger than $\frac{w}{2}$ to keep the support of the filter inside the line. We set $\sigma = s$ to get a filter with one scale parameter s . The multiscale response of the nonlinear filtering to a bar of width 10 is shown in Fig. 2. Scale integration is done by maximum projection which gives a sharp peak at the center of the bar (Fig. 2b).

Properties of the multiscale line filter

The nonlinear combination of filters that take measurements at both sides of a line profile together with the appropriate scaling result in a powerful line detection scheme.

Suppression of step edge response Depending on the direction of the slope of the edge, either the response for the edge filter E_l , or the response for E_r is negative for all x and s . The combined filter response therefore becomes $\mathcal{R}_s(x) = 0$.

Multiscale response The scale space of the filter is the 2-D function $\mathcal{R}_{\text{ScaleSp}}(s, x) = \mathcal{R}_s(x)$ (Fig. 2a). The multiscale response to the filter is the maximum over all scales s :

$$\mathcal{R}_{\text{multi}}(x) = \max_s \{ \mathcal{R}_{\text{ScaleSp}}(s, x), s_L \leq s \leq s_H \},$$

which has a maximum at $x = 0$ (Fig. 2b).

Optimal scale Given a line of width w , the scale s for which the response of the line detector has a

maximum at $x = 0$ is $s_{\text{opt}} = 0.83356 \frac{w}{2}$.

Minimum of scale at $x=0$ The scale has a local minimum at the center $x = 0$ of the multiscale response [14].

Different line profiles Figure 3 shows a roof and a Gaussian profile with the resulting multiscale response of the filter. The filter is not sensitive to the type of profile and the multiscale response still creates a sharp peak.

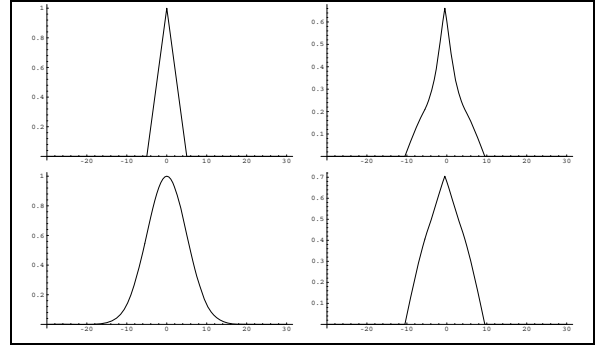


Figure 3: A roof (top) and a Gaussian (bottom) profile and the multiscale filter response (right).

Detection of noisy profiles Figure 4 shows the bar profile with added Gaussian noise with a standard deviation equal to the height of the bar. The multiscale response still shows a clear maxima near the center of the bar.

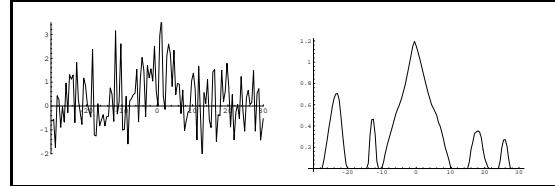


Figure 4: A bar profile of height 1 and width 10 corrupted with Gaussian noise. The multiscale response has a sharp maxima near the center of the bar.

3 The multiscale line detector in 2-D

We can extend the method for finding lines to 2-D. Let us assume that the lines have a bar profile, and are locally straight compared to the width of the line. We apply the multiscale filtering as a detection function in the direction \vec{d}_o of the profile, which is orthogonal to the line direction \vec{d}_l . The response along \vec{d}_l will be integrated by using Gaussian smoothing.

Given a direction α with $\vec{d}_o = (\cos \alpha, \sin \alpha)$, and the 2-D rotation matrix R_α we define the edge detectors at $\vec{x} = (x_1, x_2)$ as

$$E_l(\vec{x}) = R_\alpha(G'_s(x_1 + s) \cdot G_s(x_2))R_\alpha^T$$

$$E_r(\vec{x}) = R_\alpha(G'_s(x_1 - s) \cdot G_s(x_2))R_\alpha^T$$

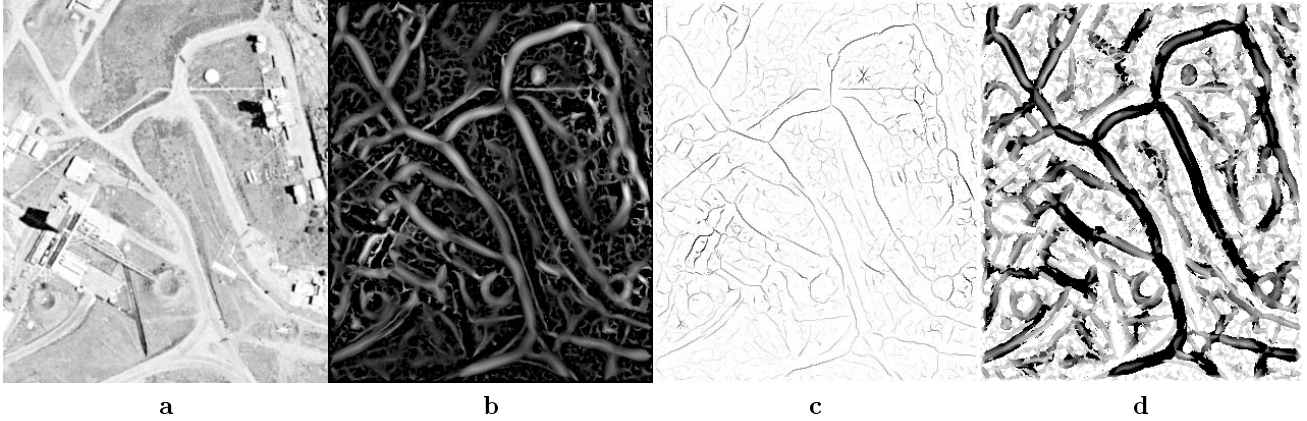


Figure 5: Detection of line-like structures in an aerial scene (a). The filter response is shown in (b). Nonmaximum suppression yields the center-lines of curvilinear structures (c). Image (d) shows the scale attributed to each point.

The variance of the integrating Gaussian function has been set equal to the scale parameter s . The 2-D multi-scale line filter response of a function $f(\vec{x})$ becomes

$$\mathcal{R}_s(\vec{x}) = \min(\text{Pos}((E_l \otimes f)(\vec{x})), \text{Pos}((E_r \otimes f)(\vec{x}))).$$

Integration of multiple orientations and multiple scales

The filter defined above is steerable in the parameters α and s [5]. We first consider the direction parameter α to find the direction which gives maximal response. Basically there are two possibilities:

- Apply the filter in a discrete number of directions, calculate the output for every direction and take the direction with the maximal value.
- Calculate the local orientation of a line structure and then steer the filter to this direction.

The second method is preferred since it avoids discretization artifacts and speeds up calculations. An estimate for the line orientation can be found by using the analysis of directional derivatives at the appropriate scales (see [3, 7]). We look for the direction where the second derivative of the function $f_s(\vec{x}) = (f \otimes G_s)(\vec{x})$ is maximal. It satisfies

$$\tan^{-1}(2\alpha) = 2 \frac{\partial^2 f}{\partial x_1 \partial x_2} \bigg/ \left(\frac{\partial^2 f}{\partial x_1^2} - \frac{\partial^2 f}{\partial x_2^2} \right).$$

The 2 solutions in $\{0, \pi\}$ give the directions \vec{d}_o and \vec{d}_l . Integration in scale-space is realized by taking the maximum across all scales, identical to the 1-D procedure.

Implementation

We can write a computationally more efficient scheme by changing the order of differentiation and convolution. We first calculate the scale-space image

f_s of f , and then take the first and second derivatives to calculate the direction and the edge filter responses:

- Calculate $f_s = f \otimes G_s$
- Calculate the gradient ∇f_s
- For all points \vec{x}
 - Calculate the direction \vec{d}_o .
 - Calculate the edge responses as:
$$\mathcal{R}_l = D_\alpha f_s(\vec{x} + s\vec{d}) = \nabla f_s(\vec{x} + s\vec{d}) \cdot \vec{d}$$

$$\mathcal{R}_r = -D_\alpha f_s(\vec{x} - s\vec{d}) = -\nabla f_s(\vec{x} - s\vec{d}) \cdot \vec{d}$$
(D_α is the first directional derivative)
 - Calculate the filter response as:
$$\min(\text{Pos}(\mathcal{R}_l), \text{Pos}(\mathcal{R}_r))$$

We apply this procedure for the range of scales in which we are interested in and take the maximal value at each point as in the 1-D case. We also keep track of the scale value at which the maximum occurred and the local orientation of the line. Non-maximum suppression is done by detecting local maxima in the direction \vec{d}_o [2].

Multiple attributes of the filter output

The multiple attributes are illustrated in Fig. 5. The filter response (5b) is proportional to the contrast of a line structure and independent of the width; the centerlines are obtained by nonmaximum suppression (5c). The corresponding scale (5d) at the position of the maximum response is proportional to the width of the line structures. Each point further is attributed by the local orientation α . These multiple attributes represent rich local information which can be queried by higher level processing. The segmentation of the ‘zebra’ image (Fig. 6) demonstrates the ability of the algorithm to simultaneously detect lines of both polarities.

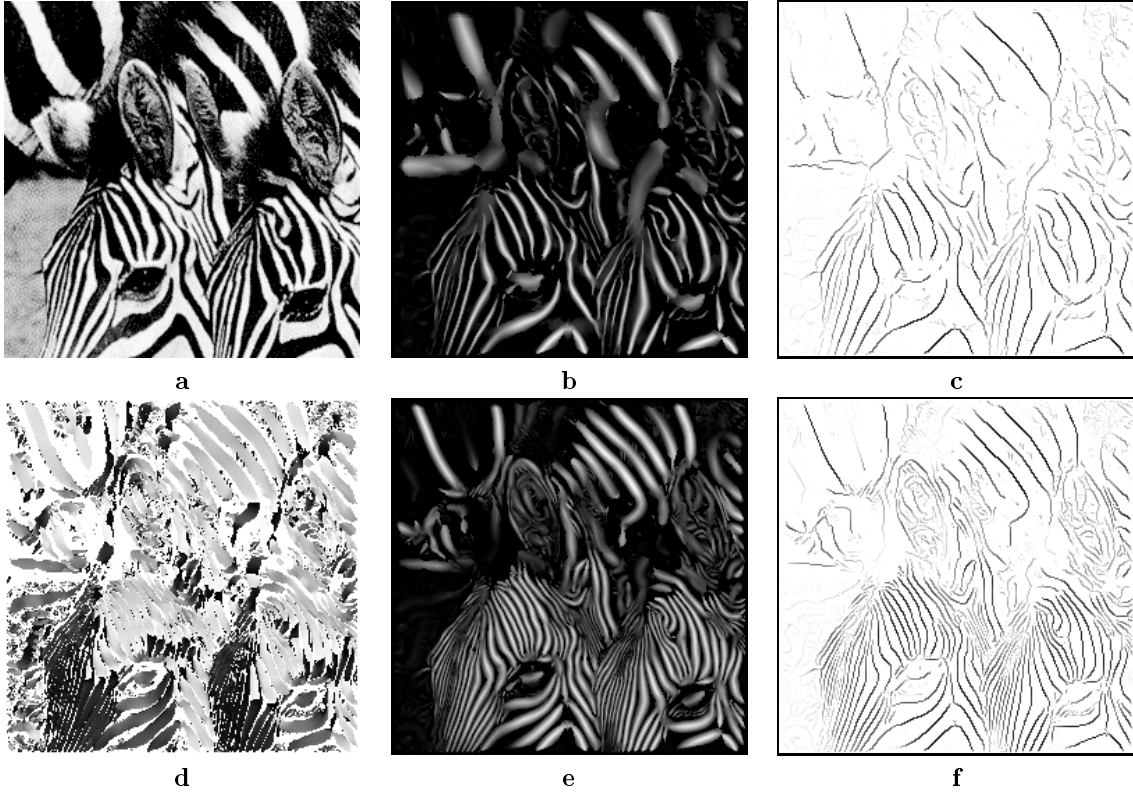


Figure 6: Detection of stripes in the ‘zebra’ image (a) using multiscale line filtering. Images (b) and (c) illustrate the multiscale response and the non-maximum suppression of dark lines. Images (e), (f) illustrate the simultaneous detection of dark and bright line structures, the corresponding orientation information is illustrated in image (d), with local orientation α encoded as a gray value.

4 Multiscale 3-D line detection in volume data

The extension of multiscale line detection to 3D is motivated by the segmentation of volume image data, e.g. by radiological magnetic resonance (MR) or computer tomographic (CT) images. In 3-D, we can use the line detection scheme for two types of features. ‘Sheet’-like structures like bone or skin tissues have a line-like profile along one direction. True curvilinear structures, 1-D manifolds in 3-D, have line-like profiles in all directions orthogonal to the line direction (Fig.7).

To find the sheet-like structures we first compute the scale image $f_s(\vec{x}) = (f \otimes G_s)(\vec{x})$ of the input data $f(\vec{x})$. The direction in which the line detection filter is applied is taken from the eigenvectors of the Hessian matrix of $f_s(\vec{x})$. We take the eigenvector associated with the largest negative eigenvalue.

For the detection of lines in 3-D, we calculate the local direction of the line from the Hessian matrix of f_s by taking the direction of the eigenvector corresponding to the smallest eigenvalue. We apply the line detection filter in the directions given by the other two

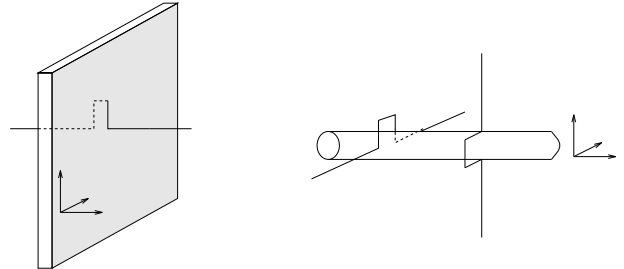


Figure 7: 3-D features with line profiles

eigenvectors as these are orthogonal to the line direction. The two values are combined by taking their minimum. So far the multiscale response could be calculated from the information at two locations, but the 3-D line has an additional degree of freedom. Our choice of evaluating the two eigenvector directions represents just one possibility.

The 3-D line detection scheme was applied to find blood vessels in 3-D magnetic resonance angiography (MRA) data of the human brain. Figure 8a and b show an axial slice of the initial data set and the multiscale response of the filter. Figure 8c presents a 3-D rendering of the segmented vasculature.

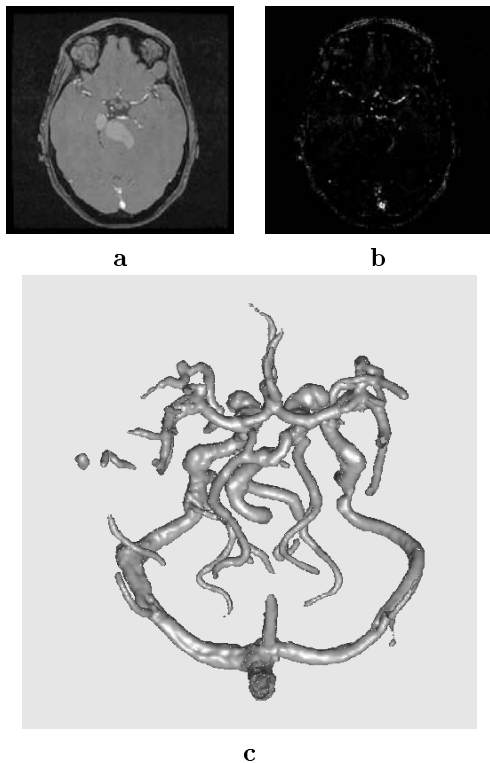


Figure 8: An axial slice from a MRA volume data presenting blood vessel as bright structures (a). The multi-scale filter response (b) marks the positions of the vessels while having only little response in the other areas. Image (c) is a 3-D surface rendering of the segmented vascular system.

5 Conclusions

We have presented a low-level segmentation scheme for curvilinear structures in 2-D and 3-D images. The nonlinear combination of linear filters gives a mono-modal response for line-like structures, thus overcoming the limitations of linear filtering [1, 2] which creates additional side-lobes for lines and also filter responses for edge-type discontinuities. We achieve *one* maximum across scale-space at a scale proportional to the width of a structure. The 2-D and 3-D extensions follow the approach of integration along the feature and detection across the feature profile. The filtering is steerable in the orientation and scale domains and creates a continuous set of self-similar filters. Integration of filter responses across scales and orientation is simplified to a maximum search.

The filter creates a rich local description of line-type structures by calculating the center position, the contrast, the width and the local direction. These multiple attributes can be queried for solving higher-level image analysis tasks.

A problem is conceptually given by the integration

scheme selecting *only one maximum* in the orientation-scale domain. Higher-order geometric structures like crossings and junctions would have to be represented by several lines in different orientations. Further, structures can have multiple meanings across scales by forming new super-structures. The problem could only be solved by processing the full orientation-scale filter space.

An extended version of this paper is available as a technical report[8].

References

- [1] J. F. Canny. Finding edges and lines in images. Technical Report 720, MIT Artificial Intelligence Laboratory, 1983.
- [2] J. F. Canny. A computational approach to edge detection. *IEEE PAMI*, 8:679–698, 1986.
- [3] D. Eberly, R. Gardner, B. Morse, S. Pizer, and C. Scharlach. Ridges for image analysis. Technical report, University of North Carolina Computer Science Department, TR93-055, 1994.
- [4] M. Fischler, J. Tenenbaum, and H. Wolf. Detection of Roads and Linear Structures in Low-Resolution Aerial Imagery Using a Multisource Knowledge Integration. *Computer Graphics and Image Processing*, 15:201–223, 1981.
- [5] W. Freeman and E. Adelson. Steerable filters for early vision, image analysis and wavelet decomposition. In *Third International Conference on Computer Vision, ICCV'90*, pages 406–415. IEEE Computer Society, Dec. 1993.
- [6] J. Gauch and S. M. Pizer. Multiresolution analysis of ridges and valleys in grey-scale images. *IEEE PAMI*, 15(6):635–646, June 1993.
- [7] R. Haralick. Ridges and valleys on digital images. *CVGIP*, 22:28–38, 1983.
- [8] T. Koller, G. Gerig, G. Székely, and D. Dettwiler. Multiscale detection of curvilinear structures in 2-D and 3-D image data. BIWI-TR 153, Communication Technology Lab, Image Science, ETH Zurich, 1994.
- [9] P. Kube. Properties of energy edge detectors. In *CVPR'92*, pages 586–591, 1992.
- [10] P. Kube and P. Perona. Scale-space properties of quadratic edge detectors. Technical Report 31, California Institute of Technology, Oct. 1993.
- [11] M. Morrone and D. Burr. Feature detection in human vision: A phase-dependent energy model. In *Proceedings of the Royal Society of London*, number 235 in B, pages 221–245, 1988.
- [12] P. Perona. Steerable-scalable kernels for edge detection and junction analysis. In G. Sandini, editor, *ECCV'92*, volume 588 of *Lecture Notes in Computer Science*, pages 3–18. Springer-Verlang, 1992.
- [13] A. Rosenfeld and M. Thurston. Edge and curve detection for visual scene analysis. *IEEE Trans. Comput.*, C-20:562–569, May 1971.
- [14] J. B. Subirana-Vilanova and K. K. Sung. Ridge detection for the perceptual organization without edges. In *ICCV'93*, pages 57–64. IEEE Computer Society Press, May 1993.